PROCEEDINGS OF SCIENCE

The coupled channel approach to the $\Lambda_c N$ - $\Sigma_c N$ system in lattice QCD

Takaya Miyamoto*
Yukawa Institute for Theoretical Physics, Kyoto University
Sakyo-ku, Kyoto 606-8502 Japan
E-mail: takaya.miyamoto@yukawa.kyoto-u.ac.jp

for HAL QCD Collaboration

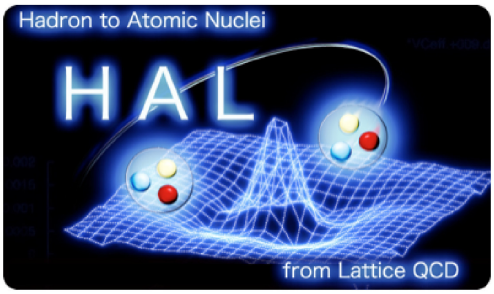

We study the interaction of s-wave $\Sigma_c N$ state in the $I(J^P) = \frac{1}{2}(1^+)$ channel. Since this state couples to the s-wave $\Lambda_c N$ $(J^P = 1^+)$ state, we have utilized the extension of the HAL QCD method to extract the coupled channel potential for the $\Lambda_c N - \Sigma_c N$ system. In our simulation, we employ gauge configurations generated by the PACS-CS Collaboration at $a = 0.0907(13)$ fm on a $L^3 \times T = 32^3 \times 64$ lattice ($La = 2.902(42)$ fm). We employ three ensembles corresponding to $m_\pi = 410, 570, 700$ MeV to study the quark mass dependence of the $\Lambda_c N - \Sigma_c N$ interactions. To reduce the discretization error coming from the heavy quark mass, we employ the relativistic heavy quark (RHQ) action for the charm quark. The phase shifts and scattering length obtained from the extracted potential matrix show that the $\Sigma_c N$ interaction is attractive at low energy stronger than the $\Lambda_c N$ interaction though no bound state at $m_\pi \geq 410$ MeV.

34th annual International Symposium on Lattice Field Theory
24-30 July 2016
University of Southampton, UK

*Speaker.

© Copyright owned by the author(s) under the terms of the Creative Commons Attribution-NonCommercial-NoDerivatives 4.0 International License (CC BY-NC-ND 4.0).

PoS(LATTICE2016)117

1. Introduction

It is interesting and important to determine the nature of interactions between nucleon and heavy baryon such as Λ_c. For example, if the $\Lambda_c N$ interaction is attractive, the net attraction between Λ_c and nucleus becomes stronger as the atomic number of the nucleus increases, so that Λ_c-nucleus can be formed. Indeed the OBEP model extended to the flavor SU(4) [1] first suggested the attractive interactions for $\Lambda_c N$ and $\Sigma_c N$ systems and thus existences of Λ_c-nuclei and Σ_c-nuclei. Some recent works have claimed that even the charmed 2-body systems have bound states[2, 3, 4]. Unfortunately, due to the lack of scattering data, one can not confirm these theoretical predictions so far. Therefore a determination of these interaction from QCD is mandatory.

Recently, an approach to investigate hadron interactions in lattice QCD has been proposed [5, 6] and extensively developed by the HAL QCD Collaboration[7, 8, 9, 10, 11, 12, 13, 14, 15]. We previously applied this method to the s-wave $\Lambda_c N$ ($J^P = 0^+$) interaction[16] and found that the $\Lambda_c N$ interaction is attractive but not strong enough to have a bound state. This weak attractive interaction might reflect an absence of one-pion exchange between Λ_c and N.

In this report, we instead consider the $\Sigma_c N$ interaction, which may have stronger attraction due to the presence of the one-pion exchange between them. In particular, we focus our attention on the $J^P = 1^+$ channel of the $\Sigma_c N$ system, since the one-pion exchange generates the tensor force, which plays an important role to form the bound deuteron for the NN system. We employ the HAL QCD method to investigate the interaction of the s-wave $\Sigma_c N$ ($J^P = 1^+$) system with $I = 1/2$. Since this system couples to the s-wave $\Lambda_c N$ ($J^P = 1^+$) system, whose total mass is lower than that of $\Sigma_c N$, we utilize the extension of the HAL QCD method[15, 17, 18] to extract the coupled channel potential for the $\Lambda_c N - \Sigma_c N$ system.

After introducing our methodology in Sec. 2 and details of numerical simulations in Sec. 3, we present our results on the coupled-channel potential for the $\Lambda_c N - \Sigma_c N$ system in the s-wave $J^P = 1^+$ state in Sec. 4.1. We also calculate the phase shift and scattering length by solving Schrödinger equartion with the extracted potential in Sec. 4.2. We give our conclusion on the nature of the $\Sigma_c N$ interaction in Sec. 5.

2. HAL QCD method

In this section, we briefly review the coupled channel HAL QCD method[17, 18]. A key quantity in the HAL QCD method is the equal-time Nambu-Bethe-Salpeter (NBS) wave function, which encodes informations of scattering phase shifts in its asymptotic behavior[17]. The NBS wave function with the total energy W_n is defined as

$$\psi^C_{W_n}(\vec{r})\mathrm{e}^{-W_n t} = \frac{1}{\sqrt{Z^{C_1}}\sqrt{Z^{C_2}}}\sum_{\vec{x}}\langle 0|B^{C_1}(\vec{r}+\vec{x},t)B^{C_2}(\vec{x},t)|B,W_n\rangle, \tag{2.1}$$

where the index C denote the flavor channel ($C = \Lambda_c N,\ \Sigma_c N$), and $B^{C_i}(\vec{x},t)$ is the local interpolating operator for the baryon C_i with its renormalization factor $\sqrt{Z^{C_i}}$. The state $|B,W_n\rangle$ stands for the QCD eigenstate for baryon number B with the relativistic energy. From the NBS wave functions, we define the non-local potentials through the following coupled-channel Schrödinger equation,

$$\left(E^C_n - H^C_0\right)\psi^C_{W_n}(\vec{r}) = \sum_{C'}\int d^3r'\, U^{C,C'}(\vec{r},\vec{r'})\psi^{C'}_{W_n}(\vec{r'}), \tag{2.2}$$

PoS(LATTICE2016)117

where $H_0^C = -\nabla^2/2\mu^C$ with the reduced mass $\mu^C = m^{C_1}m^{C_2}/(m^{C_1}+m^{C_2})$, and $E_n^C = k_n^2/2\mu^C$ is a non-relativistic energy of the C channel in the center-of-mass (CM) frame. In order to handle the non-locality of the potential, we introduce the derivative expansion of the non-local potential,

$$U(\vec{r},\vec{r'}) = (V_{\rm LO}(\vec{r}) + V_{\rm NLO}(\vec{r},\nabla) + \cdots)\,\delta^{(3)}(\vec{r}-\vec{r'}). \tag{2.3}$$

where N^{n}LO term of the local potential is $\mathscr{O}(\vec{\nabla}^n)$. At low energy, the $V_{\rm LO}$ dominates and then the coupled-channel potential matrix can be calculated by using the NBS wave functions. In the case of $\Lambda_c N - \Sigma_c N$ coupled channel, the potential matrix is extracted as

$$\begin{pmatrix} V^{\Lambda_c N,\Lambda_c N}(\vec{r}) & V^{\Lambda_c N,\Sigma_c N}(\vec{r}) \\ V^{\Sigma_c N,\Lambda_c N}(\vec{r}) & V^{\Sigma_c N,\Sigma_c N}(\vec{r}) \end{pmatrix} = \begin{pmatrix} K_{W_1}^{\Lambda_c N}(\vec{r}) & K_{W_2}^{\Lambda_c N}(\vec{r}) \\ K_{W_1}^{\Sigma_c N}(\vec{r}) & K_{W_2}^{\Sigma_c N}(\vec{r}) \end{pmatrix} \begin{pmatrix} \psi_{W_1}^{\Lambda_c N}(\vec{r}) & \psi_{W_2}^{\Lambda_c N}(\vec{r}) \\ \psi_{W_1}^{\Sigma_c N}(\vec{r}) & \psi_{W_2}^{\Sigma_c N}(\vec{r}) \end{pmatrix}^{-1}, \tag{2.4}$$

where $K_{W_n}^C(\vec{r}) \equiv \left(E_n^C - H_0^C\right)\psi_{W_n}^C(\vec{r})$.

The NBS wave functions can be extracted from the baryon four-points correlation function on the lattice defined by

$$G^{CC'}(\vec{r},t-t_0) = \sum_{\vec{x}} \langle 0|B^{C_1}(\vec{r}+\vec{x},t)B^{C_2}(\vec{x},t)\overline{\mathscr{J}_{\rm wall}^{C'}}(t_0)|0\rangle \tag{2.5}$$

$$= \sqrt{Z^{C_1}}\sqrt{Z^{C_2}}\sum_n \psi_{W_n}^C(\vec{r})e^{-W_n(t-t_0)}A_n^{C'} + \cdots, \tag{2.6}$$

with $A_n^{C'} = \langle B, W_n|\overline{\mathscr{J}_{\rm wall}^{C'}}(0)|0\rangle$, where $\overline{\mathscr{J}_{\rm wall}^{C'}}(t_0)$ stands for the zero momentum wall source operator which creates two-baryon states in channel C'. The ellipses denote inelastic contributions coming from channels above C and C'. The ground state of the NBS wave function can be extracted for sufficiently large t, where contributions from all excited states can be neglected. Since the signal-to-noise ratio of the baryon four-points correlation function decreases exponentially for larger t, however, we instead employ the time-dependent HAL QCD method[9], which does not require the grand state saturation for the extraction of potentials. With the approximation neglecting $\mathscr{O}(k^4)$ contributions, the normalized baryon four-points correlation function $R^{CC'}(\vec{r},t-t_0) \equiv G^{CC'}(\vec{r},t-t_0)/\mathrm{e}^{-(m^{C_1}+m^{C_2})(t-t_0)}$ satisfies following relation for a sufficiently large t where contributions from inelastic states above C and C' channels can be neglected.

$$\left(-\frac{\partial}{\partial t} + \left[\frac{1+(\delta^C)^2}{8\mu^C}\right]\frac{\partial^2}{\partial t^2} - H_0^C\right)R^{CC'}(\vec{r},t-t_0) = \sum_{C''}\int d^3r'\,\Delta^{C,C''}U^{C,C''}(\vec{r},\vec{r'})R^{C''C'}(\vec{r'},t-t_0), \tag{2.7}$$

where δ^C denotes $\delta^C = (m^{C_1}-m^{C_2})/(m^{C_1}+m^{C_2})$ and $\Delta^{C,C''}$ is defined as

$$\Delta^{C,C''} = \frac{\sqrt{Z^{C_1}}\sqrt{Z^{C_2}}\exp[-(m^{C_1''}+m^{C_2''})(t-t_0)]}{\sqrt{Z^{C_1''}}\sqrt{Z^{C_2''}}\exp[-(m^{C_1}+m^{C_2})(t-t_0)]}. \tag{2.8}$$

In the case of the $\Lambda_c N - \Sigma_c N$ system, the potential matrix at the LO of the velocity expansion is extracted as

$$\begin{pmatrix} V^{\Lambda_c N,\Lambda_c N} & \Delta^{\Lambda_c N,\Sigma_c N}V^{\Lambda_c N,\Sigma_c N} \\ \Delta^{\Sigma_c N,\Lambda_c N}V^{\Sigma_c N,\Lambda_c N} & V^{\Sigma_c N,\Sigma_c N} \end{pmatrix} = \begin{pmatrix} \mathscr{K}^{\Lambda_c N,\Lambda_c N} & \mathscr{K}^{\Lambda_c N,\Sigma_c N} \\ \mathscr{K}^{\Sigma_c N,\Lambda_c N} & \mathscr{K}^{\Sigma_c N,\Sigma_c N} \end{pmatrix} \begin{pmatrix} R^{\Lambda_c N,\Lambda_c N} & R^{\Lambda_c N,\Sigma_c N} \\ R^{\Sigma_c N,\Lambda_c N} & R^{\Sigma_c N,\Sigma_c N} \end{pmatrix}^{-1}, \tag{2.9}$$

PoS(LATTICE2016)117

Table 1: The hadron masses calculated on PACS-CS configurations.

Hadron	Ensemble 1	Ensemble 2	Ensemble 3
π	702 (2) MeV	570 (1) MeV	412 (2) MeV
N	1581 (6) MeV	1399 (9) MeV	1215 (9) MeV
Λ_c	2685 (3) MeV	2555 (5) MeV	2434 (6) MeV
Σ_c	2780 (5) MeV	2674 (7) MeV	2575 (9) MeV

where we omit $(\vec{r}, t-t_0)$ for simplicity and $\mathscr{K}^{CC'}$ is defined as

$$\mathscr{K}^{CC'}(\vec{r}, t-t_0) = \left(-\frac{\partial}{\partial t} + \left[\frac{1+(\delta^C)^2}{8\mu^C} \right] \frac{\partial^2}{\partial t^2} - H_0^C \right) R^{CC'}(\vec{r}, t-t_0). \tag{2.10}$$

3. Lattice setup

For numerical simulations, we have employed the $2+1$ flavor full QCD configurations generated by the PACS-CS Collaboration[19] with the renormalization-group improved Iwasaki gauge action and a nonperturbatively $\mathscr{O}(a)$ improved Wilson quark action. The lattice size is $L^3 \times T = 32^3 \times 64$ and the lattice spacing is $a = 0.0907(13)$ fm (physical lattice size is $La = 2.902(42)$ fm). In order to see the quark mass dependence of the potential, we have employed three ensembles of gauge configurations correspond to $m_\pi = 702(2),\ 570(1),\ 412(2)$ MeV. We employed the relativistic heavy quark (RHQ) action[20] to reduce the leading $\mathscr{O}((m_Q a)^n)$ discretization errors with charm quark mass m_Q. We employ the RHQ parameters determined in Ref.[21] so as to reproduce η_C (2983) and J/ψ (3097) masses in nature. Hadron masses calculated on these configurations are given in Table 1.

4. Numerical results

4.1 Potentials

In Fig.1, we show the numerical results of the s-wave $\Lambda_c N - \Sigma_c N$ coupled-channel potential matrix in the $J^P = 1^+$ state. Each of the figures contain results of potentials for three different pion masses. They correspond to so-called effective central potentials in which the effects of tensor forces are implicitly included. In Fig.1, we observe a strong attraction in the $V_{\Sigma_c N, \Sigma_c N}$ potential, which might be a manifestation of the one-pion exchange, while the $V_{\Lambda_c N, \Lambda_c N}$ potential, which is consistent with that from the single-channel analysis[16], remains weak. Both diagonal potentials have strong pion-mass dependences. On the other hand, the strength of the off-diagonal potentials is weak and they are almost independent of pion masses.

4.2 Phase shift and scattering length

Once we obtain the potential matrix, we can calculate the phase shifts of $\Lambda_c N$ and $\Sigma_c N$ in the infinite volume. For this purpose, we employ the four-ranges Gaussian for the fit function given by

$$V(r) = \sum_{n=1}^{4} a_n e^{-\left(\frac{r}{b_n}\right)^2}. \tag{4.1}$$

PoS(LATTICE2016)117

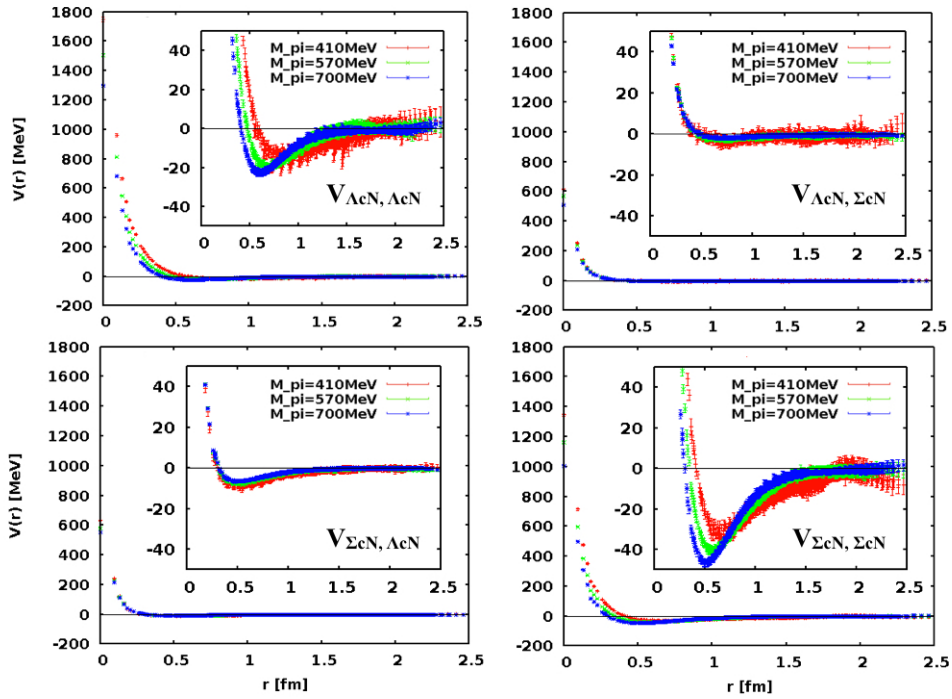

Figure 1: The s-wave $\Lambda_c N - \Sigma_c N$ coupled-channel potential matrix in the $J^P = 1^+$ state. Different colors represent different pion masses. The time separation between sink and source is $t - t_0 = 10$.

With the fitted function, we solve the coupled-channel Schrödinger equation and we extract the S matrix from the asymptotic form of the wave function as

$$\begin{pmatrix} \psi_{\Lambda_c N}(r) \\ \psi_{\Sigma_c N}(r) \end{pmatrix} = \begin{pmatrix} h_0^{(1)}(kr) & 0 \\ 0 & h_0^{(1)}(qr) \end{pmatrix} \begin{pmatrix} C_{\Lambda_c N} \\ C_{\Sigma_c N} \end{pmatrix} + \begin{pmatrix} h_0^{(2)}(kr) & 0 \\ 0 & h_0^{(2)}(qr) \end{pmatrix} \begin{pmatrix} S_{\Lambda_c N,\Lambda_c N} & S_{\Lambda_c N,\Sigma_c N} \\ S_{\Sigma_c N,\Lambda_c N} & S_{\Sigma_c N,\Sigma_c N} \end{pmatrix} \begin{pmatrix} C_{\Lambda_c N} \\ C_{\Sigma_c N} \end{pmatrix}, \tag{4.2}$$

where $h_l^{(1)}(kr)$ and $h_l^{(2)}(kr)$ are Spherical Hankel functions for the angular momentum l, and $C_{\{\Lambda_c N,\ \Sigma_c N\}}$ are constants determined from the boundary condition. Here k (q) represents an absolute value of the relative momentum in the CM frame for the $\Lambda_c N$ ($\Sigma_c N$) channel. The definition of the phase shift for the coupled channel system is given in Ref.[22] as

$$\begin{pmatrix} S_{\Lambda_c N,\Lambda_c N} & S_{\Lambda_c N,\Sigma_c N} \\ S_{\Sigma_c N,\Lambda_c N} & S_{\Sigma_c N,\Sigma_c N} \end{pmatrix} \equiv \begin{pmatrix} e^{i\bar{\delta}_{\Lambda_c N}} & 0 \\ 0 & e^{i\bar{\delta}_{\Sigma_c N}} \end{pmatrix} \begin{pmatrix} \cos 2\bar{\theta} & i\sin 2\bar{\theta} \\ i\sin 2\bar{\theta} & \cos 2\bar{\theta} \end{pmatrix} \begin{pmatrix} e^{i\bar{\delta}_{\Lambda_c N}} & 0 \\ 0 & e^{i\bar{\delta}_{\Sigma_c N}} \end{pmatrix}, \tag{4.3}$$

where $\bar{\delta}$ is so-called the bar phase shift and $\bar{\theta}$ is the mixing angle. To retain the unitarity of the S-matrix, two off-diagonal elements of the potential matrix are replaced by their average, though the result obtained with the original potential matrix does not change within statistical errors.

Fig.2 shows the phase shifts of the $\Lambda_c N$ and the $\Sigma_c N$ channels on the three ensembles. In Fig.2, we find that there are no bound state for both $\Lambda_c N$ and $\Sigma_c N$ channels at all pion masses, even though the attraction of the $\Sigma_c N$ channel at low energy is stronger than that of the $\Lambda_c N$ channel. We also find that the mixing angle between $\Lambda_c N$ and $\Sigma_c N$ is small ($|\bar{\theta}| < 3^\circ$). This observation might

PoS(LATTICE2016)117

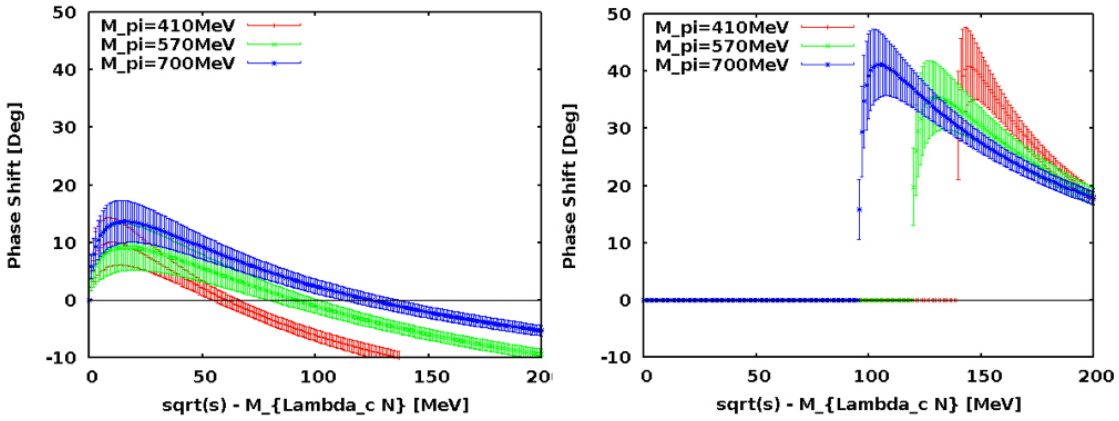

Figure 2: The phase shifts of s-wave $\Lambda_c N$(left) and s-wave $\Sigma_c N$(right) in the $J^P = 1^+$ state. Different colors represent different pion masses.

Table 2: The scattering lengths calculated by using Eq.(4.4).

m_π	702(2) MeV	570(1) MeV	412(2) MeV
$a_{\Lambda_c N}$	0.46 (18) fm	0.29 (13) fm	0.29 (16) fm
$a_{\Sigma_c N}$	2.71 (97) fm	2.02 (86) fm	4.00 (1.97) fm

be understood from the fact that the mass splitting between the $\Lambda_c N$ and the $\Sigma_c N$ is large. Since the two channels are almost independent each other due to the small mixing and thus can be regarded as two single channels, we define the scattering lengths of $\Lambda_c N$ ($\Sigma_c N$) as

$$a_{\Lambda_c N} = \lim_{k\to 0} \frac{\tan\bar{\delta}_{\Lambda_c N}(k)}{k}, \qquad a_{\Sigma_c N} = \lim_{q\to 0} \frac{\tan\bar{\delta}_{\Sigma_c N}(q)}{q}, \tag{4.4}$$

and results are given in Table 2. It seems that the scattering length of $\Sigma_c N$ increases as the pion mass decreases though statistical errors are large, while the one of $\Lambda_c N$ is almost independent of the pion masses.

5. Summary

We have investigated the s-wave $\Sigma_c N$ interaction in the $I(J^P) = \frac{1}{2}(1^+)$ state using the $\Lambda_c N - \Sigma_c N$ coupled channel potentials obtained by the extension of the HAL QCD method. In order to study the pion mass dependence, we have employed three ensembles of gauge configurations generated at $m_\pi = 702(2), 570(1), 412(2)$ MeV. Results of the potential matrix show that the $\Sigma_c N$ interaction is attractive at low energy stronger than the $\Lambda_c N$ interaction, probably due to the one-pion exchange. We have also observed weak off-diagonal elements of the potential matrix. The phase shifts and mixing angle extracted by solving Schrödinger equation in the infinite volume with the obtained potentials show that that the $\Sigma_c N$ channel does not have the two-body bound state at $m_\pi \geq 410$ MeV, even though the net attraction of the $\Sigma_c N$ channel is stronger than that of the $\Lambda_c N$

PoS(LATTICE2016)117

channel. The mixing angle between $\Lambda_c N$ and $\Sigma_c N$ channel also indicates a small coupling between the two.

In future, we will calculate the s-wave $\Sigma_c N$ interaction in the $I(J^P) = \frac{1}{2}(0^+)$ state to investigate the spin-dependence. We will also calculate the interaction of the $\Sigma_c N$ system at physical pion mass.

Acknowledgments

We thank the PACS-CS Collaboration for providing us their $2+1$ flavor gauge configurations [19]. Numerical computations of this work have been carried out by the KEK supercomputer system (BG/Q), [Project number : 15/16-12].

References

[1] C. B. Dover and S. H. Kahana, Phys. Rev. Lett. **39** (1977) 1506.

[2] Y. R. Liu and M. Oka, Phys. Rev. **D85** (2012) 014015 [arXiv:1103.4624 [hep-ph]].

[3] H. Huang, J. Ping and F. Wang, Phys. Rev. **C87** (2013) 034002.

[4] S. Maeda, M. Oka, A. Yokota, E. Hiyama and Y. R. Liu, Prog. Theor. Exp. Phys. **2016** (2016) 023D02. [arXiv:1509.02445 [nucl-th]].

[5] N. Ishii, S. Aoki and T. Hatsuda, Phys. Rev. Lett. **99** (2007) 022001 [nucl-th/0611096].

[6] S. Aoki, T. Hatsuda and N. Ishii, Prog. Theor. Phys. **23** (2010) 89 [arXiv:0909.5585 [hep-lat]].

[7] S. Aoki *et al*. [HAL QCD Collaboration], Prog. Theor. Exp. Phys. **2012** (2012) 01A105 [arXiv:1206.5088 [hep-lat]].

[8] T. Inoue *et al*. [HAL QCD Collaboration], Phys. Rev. Lett. **106** (2011) 162002 [arXiv:1012.5928 [hep-lat]].

[9] N. Ishii *et al*. [HAL QCD Collaboration], Phys. Lett. **B712** (2012) 437 [arXiv:1203.3642 [hep-lat]].

[10] T. Doi *et al*. [HAL QCD Collaboration], Prog. Theor. Phys. **127** (2012) 723.

[11] T. Inoue *et al*. [HAL QCD Collaboration], Phys. Rev. Lett. **111** (2013) 112503 [arXiv:1307.0299 [hep-lat]].

[12] Y. Ikeda *et al*. [HAL QCD Collaboration], Phys. Lett. **B729** (2014) [arXiv:1311.6214 [hep-lat]].

[13] K. Murano *et al*. [HAL QCD Collaboration], Phys. Lett. **B735** (2014) 19 [arXiv:1305.2293 [hep-lat]].

[14] K. Sasaki *et al*. Prog. Theor. Exp. Phys. (2015) 113B01 [arXiv:1504.01717 [hep-lat]].

[15] Y. Ikeda *et al*. Phys. Rev. Lett. **117**, 242001, (2016) [arXiv:1602.03465 [hep-lat]].

[16] T. Miyamoto for HAL QCD Collaboration, PoS (**LATTICE 2015**) 090 (2016) [arXiv:1602.07797 [hep-lat]].

[17] S. Aoki *et al*. [HAL QCD Collaboration], Proc. Jpn. Acad., Ser. B, **87** (2011) 509 [arXiv:1106.2281 [hep-lat]].

[18] S. Aoki, B. Charron, T. Doi, T. Hatsuda, T. Inoue and N. Ishii, Phys. Rev. D **87** (2013) 034512 [arXiv:1212.4896 [hep-lat]].

[19] PACS-CS Collaboration: S. Aoki, *et al*., Phys. Rev. D **79** (2009) 034503.

[20] S. Aoki, Y. Kuramashi and S. Tominaga, Prog. Theor. Phys **109** (2003) 383. [arXiv:hep-lat/0107009].

[21] Y. Namekawa, *et al*. (PACS-CS Collaboration), Phys. Rev. D **87**, 094512 [arXiv:1301.4743 [hep-lat]].

[22] H. Stapp, T. J. Ypsilantis and N. Metropolis, Phys. Rev. **105** (1957) 302.

PoS(LATTICE2016)117